

Perfect Recovery Conditions For Non-Negative Sparse Modeling

Yuki Itoh, *Student Member, IEEE*, Marco F. Duarte, *Senior Member, IEEE*,
and Mario Parente, *Senior Member, IEEE*

Abstract—Sparse modeling has been widely and successfully used in many applications such as computer vision, machine learning, and pattern recognition and, accompanied with those applications, significant research has studied the theoretical limits and algorithm design for convex relaxations in sparse modeling. However, only little has been done for theoretical limits of non-negative versions of sparse modeling. The behavior is expected to be similar as the general sparse modeling, but a precise analysis has not been explored. This paper studies the performance of non-negative sparse modeling, especially for non-negativity constrained and ℓ_1 -penalized least squares, and gives an exact bound for which this problem can recover the correct signal elements. We pose two conditions to guarantee the correct signal recovery: minimum coefficient condition (MCC) and non-linearity vs. subset coherence condition (NSCC). The former defines the minimum weight for each of the correct atoms present in the signal and the latter defines the tolerable deviation from the linear model relative to the positive subset coherence (PSC), a novel type of “coherence” metric. We provide rigorous performance guarantees based on these conditions and experimentally verify their precise predictive power in a hyperspectral data unmixing application.

Index Terms—sparse modeling, sparse regression, sparse recovery, non-negative constraint, lasso, recovery conditions, hyperspectral unmixing.

1 INTRODUCTION

Sparse modeling has achieved significant recognition in a variety of research areas such as signal processing, machine learning, computer vision, and pattern recognition. Sparse models refer to the formulation of a signal of interest (or an approximation of it) as the linear combination of a small number of elements (known as atoms) drawn from a so-called sparsity dictionary (or dictionary for short). The *sparse recovery* problem refers to the identification of the relevant dictionary atoms for a particular signal of interest. Sparse modeling and recovery has a rich history in signal processing, and has received significant attention recently due to the emergence of compressed sensing [1], [2], a framework for compressed signal acquisition that leverages sparse modeling.

We can further restrict the coefficients of the atoms to be non-negative. In general, non-negativity is advantageous as it makes the model parameters more interpretable. For instance, Lee and Seung present non-negative matrix factorization [3], which can learn a part-based representation of faces or documents. Just adding non-negativity constraints on a linear model to decompose spectral data gives the model coefficients the meaning of fractional abundances [4]. Non-negative constraints have been applied to independent component analysis in face recognition tasks [5].

Many approaches have combined non-negativity and sparse modeling. By adding non-negative constraints, several researchers [6], [7] refined the performance of applying sparse modeling on a face recognition task obtained by

Wright et al. [8]. Non-negativity constrained least squares (NCLS) has been traditionally used, sometimes accompanied with abundance sum-to-one constraints, to extract the spectral components from hyperspectral pixels e.g. [4], a process called *spectral unmixing*. Recently, NCLS has been combined with sparsity with improvements in the unmixing performance [9], [10]. Other examples of combining non-negativity and sparse modeling can be found in astronomical imaging [11] and proteomics [12].

This paper investigates some theoretical aspects of non-negative sparse modeling. Many works have investigated the theory of sparse modeling [13], [14], [15], [16], [17], [18], [19], [20], but all of them are devoted to *modeling in the absence of noise*, focusing on problems such as the equivalence between the extraction of the most compact representation and convex relaxation problems, or uniqueness of the solution. The theoretical aspects of the non-negativity constrained version of lasso [21], which takes noise into consideration, have not been explored and will be the focus of our attention.

We will investigate the conditions for successful reconstruction — or regression — of a signal using non-negative lasso by expanding previous analyses on the general lasso problem. Some of these studies consider dictionaries drawn according to a random distribution [22]. Others assume an arbitrary dictionary and pose conditions for successful regression that require a combinatorial amount of computation: examples include the spark, restricted isometry property, the restricted eigenvalue property, and the irrepresentable condition [2], [23], [24], [25], [26]. It is possible to relax the computational complexity of the verification process, using tools such as *coherence* [23], [27], [28], [29], [30]; however, this framework considers all possible com-

- Y. Itoh, M. F. Duarte, and M. Parente are with the Department of Electrical and Computer Engineering, University of Massachusetts, Amherst, MA, 01003.
E-mail: {yitoh,mduarte,mparente}@umass.edu

binations of atoms simultaneously, and therefore is found to often give very conservative assessments of regression performance.

This paper follows the line of Tropp’s work [30]. In contrast to the references above, Tropp has performed an analysis based on the so-called *exact recovery condition* (ERC), which provides conditions on successful reconstruction when the set of atoms involved is known in advance. The ERC can be easily computed and is compatible with well-known optimization-based and iterative greedy algorithms for sparse signal recovery and regression, and so it appears well-poised for the analysis of non-negative versions. Furthermore, because the ERC is focused on sparse signals featuring a specific support (i.e., a set of indices for the signal’s nonzero entries), its guarantees are less pessimistic than those provided by alternative approaches, which consider success for all sparse signals simultaneously, regardless of their support. Nonetheless, one could conceivably argue that restricting the set of signals of interest to a fixed support with non-negative entries may provide guarantees that are even closer to the actual performance of non-negative sparse recovery. Thus, our goal is to formulate adaptations to the ERC framework that also account for the non-negativity constraint in the problem.

1.1 Problem description

Throughout this paper, we assume a linear model with non-negative coefficients,

$$\mathbf{y} = \mathbf{A}\mathbf{x} + \mathbf{e} \quad (\mathbf{x} \succeq \mathbf{0}) \quad (1)$$

where $\mathbf{y} \in \mathbb{R}^L$ is an observation vector, $\mathbf{A} \in \mathbb{R}^{L \times N}$ is a dictionary matrix where the components \mathbf{a}_j ($j = 1, \dots, N$), called atoms, are stored in its columns, $\mathbf{x} \in \mathbb{R}^N$ is a non-negative coefficient vector, $\mathbf{e} \in \mathbb{R}^L$ is an error vector, and \succeq (and its variants) denote element-wise inequality. Based on this model, we consider the problem of inferring atoms contributing the observation. In particular, we focus on the next partially Lagrangian form of non-negative lasso (PL-NLasso),

$$\begin{aligned} & \underset{\mathbf{x}}{\text{minimize}} && \frac{1}{2} \|\mathbf{y} - \mathbf{A}\mathbf{x}\|_2^2 + \gamma \|\mathbf{x}\|_1 \\ & \text{subject to} && \mathbf{x} \succeq \mathbf{0}, \end{aligned} \quad (2)$$

where γ is a positive constant that controls the degree of sparsity.

1.2 Contribution of this paper

The main contribution of this paper is the derivation of model recovery conditions (MRC) for the PL-NLasso problem. The MRCs allow us to predict if the correct atoms are identifiable via the PL-NLasso given a signal model for a specific set of atoms with noise or non-linearity. Our MRCs includes an approximately perfect MRC for the PL-NLasso that practically meets both necessity and sufficiency. Although the approximately perfect MRC is imperfect in a rigorous mathematical sense, it is quite powerful and in our experiments provides perfect prediction of the performance of PL-NLasso. We also show some simplified variants of the approximately perfect MRC. Those MRCs are considered as customizations of Tropp’s work [30] and are rigorously

proved mathematically. Our criterion for perfect identification is that only all of the atoms present are selected by the algorithm (i.e., no missed atoms and no false alarms), without consideration for accuracy of the coefficient values involved.

We will also show how our theorem can be used in real applications. Our theorem can predict how often PL-NLasso succeeds in selecting correct atoms in the presence of deviations from the noiseless linear model, including measurement nonlinearities, bias, and noise. Experiments show that the approximately perfect MRC practically gives perfect assessment of the performance of PL-NLasso.

1.3 Mathematical notation

We specify the mathematical notation used in this paper. The support of $\mathbf{x} \in \mathbb{R}^N$ is the set of the indices associated with the non-zero elements of \mathbf{x} , denoted by $\text{supp}(\mathbf{x})$. $\mathcal{R}(\mathbf{X})$ is the range of the matrix \mathbf{X} . \mathbf{M}^\top , \mathbf{M}^{-1} , and \mathbf{M}^\dagger denote the transpose, inverse, and pseudoinverse of the matrix \mathbf{M} , respectively. $\|\mathbf{M}\|_{\infty, \infty}$ is an (∞, ∞) matrix operator norm and gives the maximum ℓ_1 -norm of the row vectors of \mathbf{M} .

We denote a subset of the column indices of $\mathbf{A} \in \mathbb{R}^{L \times N}$ by $\Lambda \subseteq \{1, 2, \dots, N\}$, and the subdictionary that are composed of atoms associated with indices in Λ by \mathbf{A}_Λ . Note that all of the theorems are discussed on a subset Λ of the column indices as Tropp [30] did. For any coefficient vector $\mathbf{x} \in \mathbb{R}^N$ defined in (1), we denote the vector composed of the elements of \mathbf{x} indexed by Λ by \mathbf{x}_Λ . We also denote the whole column index set $\Omega = \{1, 2, \dots, N\}$, and the complement of Λ by $\Lambda^c = \Omega \setminus \Lambda$ where \setminus is the difference of two sets.

1.4 Organization of this paper

The rest of this paper is organized as follows. Section 2 introduces a sufficient MRC shown in our previous work [31]. Section 3 demonstrates several MRCs for PL-NLasso of varying tightness. Section 4 illustrates an application of our MRCs to a hyperspectral unmixing task and Section 5 concludes this paper.

2 PREVIOUS WORK

We start our discussion with our previous work [31], which introduced a sufficient MRC to guarantee correct model recovery using PL-NLasso. The previous work stands on the work by Tropp [30] and depends on the exact recovery coefficient (ERC), defined by

$$\text{ERC}(\Lambda) := 1 - \max_{n \notin \Lambda} \|\mathbf{A}_\Lambda^\dagger \mathbf{a}_n\|_1. \quad (3)$$

Note that it is implicitly assumed that the columns of \mathbf{A}_Λ are linearly independent so that the pseudoinverse exists. When the columns of \mathbf{A} have unit ℓ_2 norm, the condition considers the minimum angle between atoms outside of Λ and the subspace spanned by \mathbf{A}_Λ . Intuitively, a larger ERC is preferred because it reduces correlation between \mathbf{A}_Λ and atoms outside the set. The following theorem provides performance guarantees for the lasso that are specific to a particular support Λ . Tropp considers the general lasso problem

$$\underset{\mathbf{x}}{\text{minimize}} \quad \frac{1}{2} \|\mathbf{y} - \mathbf{A}\mathbf{x}\|_2^2 + \gamma \|\mathbf{x}\|_1 \quad (4)$$

and derived a theorem to guarantee the performance of this problem:

Theorem 2.1. [30, Theorem 8] Let Λ index a linearly independent collection of columns of \mathbf{A} for which $\text{ERC}(\Lambda) \geq 0$. Suppose that \mathbf{y} is an input signal whose ℓ_2 best approximation $\mathbf{y}_\Lambda = \mathbf{A}_\Lambda \mathbf{A}_\Lambda^\dagger \mathbf{y}$ over \mathbf{A}_Λ satisfies the correlation condition

$$\|\mathbf{A}^\top(\mathbf{y} - \mathbf{y}_\Lambda)\|_\infty \leq \gamma \text{ERC}(\Lambda). \quad (5)$$

Let \mathbf{x}^* be the solution of the lasso (4) with parameter γ . We may conclude the following.

- $\text{supp}(\mathbf{x}^*)$, is contained in Λ ;
- the distance between \mathbf{x}^* and the optimal coefficient vector $\mathbf{c}_\Lambda = \mathbf{A}_\Lambda^\dagger \mathbf{y}$ (appropriately zero-padded) satisfies

$$\|\mathbf{x}_\Lambda^* - \mathbf{c}_\Lambda\|_\infty \leq \gamma \|(\mathbf{A}_\Lambda^\top \mathbf{A}_\Lambda)^{-1}\|_{\infty, \infty}; \quad (6)$$

- and $\text{supp}(\mathbf{x}^*)$ contains the indices $\lambda \in \Lambda$ for which

$$|\mathbf{c}_\Lambda(\lambda)| > \gamma \|(\mathbf{A}_\Lambda^\top \mathbf{A}_\Lambda)^{-1}\|_{\infty, \infty}. \quad (7)$$

Using the theorem above, we derived the following theorem to guarantee the performance of PL-NLasso:

Theorem 2.2. [31, Theorem 2] Assume a signal model $\mathbf{y} = \mathbf{A}\mathbf{x}^{\text{true}} + \mathbf{e}$, where the abundance vector $\mathbf{x}^{\text{true}} \succeq \mathbf{0}$, $\Lambda = \text{supp}(\mathbf{x}^{\text{true}})$ indexes a linearly independent collection of columns of \mathbf{A} , and \mathbf{e} represents the effect of noise or nonlinear distortion during acquisition. Let $\hat{\mathbf{x}}$ be the solution of PL-NLasso with parameter γ . If the noise \mathbf{e} obeys

$$\|\mathbf{A}^\top \mathbf{P}_\Lambda^\perp \mathbf{e}\|_\infty \leq \gamma \text{ERC}(\Lambda) \quad (8)$$

where \mathbf{P}_Λ^\perp is the projector onto the orthogonal complement of $\mathcal{R}(\mathbf{A}_\Lambda)$, and

$$\mathbf{x}_\Lambda^{\text{true}} \succ \gamma \|(\mathbf{A}_\Lambda^\top \mathbf{A}_\Lambda)^{-1}\|_{\infty, \infty} - \mathbf{A}_\Lambda^\dagger \mathbf{e}, \quad (9)$$

then we have that $\text{supp}(\hat{\mathbf{x}}) = \Lambda$.

Proof: We begin by considering the solution \mathbf{x}^* to the lasso with parameter γ for the input \mathbf{y} . By applying Theorem 2.1 and seeing that

$$\begin{aligned} & \|\mathbf{A}^\top(\mathbf{y} - \mathbf{y}_\Lambda)\|_\infty \\ &= \|\mathbf{A}^\top(\mathbf{y} - \mathbf{A}_\Lambda \mathbf{A}_\Lambda^\dagger \mathbf{y})\|_\infty \\ &= \|\mathbf{A}^\top(\mathbf{A}\mathbf{x}^{\text{true}} + \mathbf{e} - \mathbf{A}_\Lambda \mathbf{A}_\Lambda^\dagger (\mathbf{A}\mathbf{x}^{\text{true}} + \mathbf{e}))\|_\infty \\ &= \|\mathbf{A}^\top(\mathbf{A}_\Lambda \mathbf{x}_\Lambda^{\text{true}} + \mathbf{e} - \mathbf{A}_\Lambda \mathbf{A}_\Lambda^\dagger (\mathbf{A}_\Lambda \mathbf{x}_\Lambda^{\text{true}} + \mathbf{e}))\|_\infty \\ &= \|\mathbf{A}^\top(\mathbf{A}_\Lambda \mathbf{x}_\Lambda^{\text{true}} + \mathbf{e} - \mathbf{A}_\Lambda \mathbf{x}_\Lambda^{\text{true}} - \mathbf{A}_\Lambda \mathbf{A}_\Lambda^\dagger \mathbf{e})\|_\infty \\ &= \|\mathbf{A}^\top(\mathbf{e} - \mathbf{A}_\Lambda \mathbf{A}_\Lambda^\dagger \mathbf{e})\|_\infty = \|\mathbf{A}^\top(\mathbf{I} - \mathbf{A}_\Lambda \mathbf{A}_\Lambda^\dagger) \mathbf{e}\|_\infty \\ &= \|\mathbf{A}^\top \mathbf{P}_\Lambda^\perp \mathbf{e}\|_\infty, \end{aligned} \quad (10)$$

we have that (10) and (8) imply (5). Thus, we obtain the following results:

- The support of \mathbf{x}^* , $\text{supp}(\mathbf{x}^*)$, is contained in Λ , and
- the distance between \mathbf{x}^* and the optimal coefficient vector

$$\begin{aligned} \mathbf{c}_\Lambda &= \mathbf{A}_\Lambda^\dagger \mathbf{y} = \mathbf{A}_\Lambda^\dagger (\mathbf{A}\mathbf{x}^{\text{true}} + \mathbf{e}) = \mathbf{A}_\Lambda^\dagger (\mathbf{A}_\Lambda \mathbf{x}_\Lambda^{\text{true}} + \mathbf{e}) \\ &= \mathbf{x}_\Lambda^{\text{true}} + \mathbf{A}_\Lambda^\dagger \mathbf{e} \end{aligned}$$

(appropriately zero-padded) satisfies

$$\|\mathbf{x}^* - \mathbf{x}_\Lambda^{\text{true}} - \mathbf{A}_\Lambda^\dagger \mathbf{e}\|_\infty \leq \gamma \|(\mathbf{A}_\Lambda^\top \mathbf{A}_\Lambda)^{-1}\|_{\infty, \infty}. \quad (11)$$

The result (11) implies that for each $n \in \Lambda$ we have

$$\begin{aligned} |\mathbf{x}^*(n) - (\mathbf{x}^{\text{true}}(n) + \mathbf{w}(n))| &\leq \gamma \|(\mathbf{A}_\Lambda^\top \mathbf{A}_\Lambda)^{-1}\|_{\infty, \infty}, \\ -\gamma \|(\mathbf{A}_\Lambda^\top \mathbf{A}_\Lambda)^{-1}\|_{\infty, \infty} &\leq \mathbf{x}^*(n) - \mathbf{x}^{\text{true}}(n) - \mathbf{w}(n), \\ \mathbf{x}^{\text{true}}(n) + \mathbf{w}(n) - \gamma \|(\mathbf{A}_\Lambda^\top \mathbf{A}_\Lambda)^{-1}\|_{\infty, \infty} &\leq \mathbf{x}^*(n), \end{aligned}$$

where we denote $\mathbf{w} = \mathbf{A}_\Lambda^\dagger \mathbf{e}$. Thus, from the condition (9), we have that $\mathbf{x}^*(n) > 0$ for all $n \in \Gamma$, which implies that $\Lambda \subseteq \text{supp}(\mathbf{x}^*)$. Furthermore, since $\text{supp}(\mathbf{x}^*) \subseteq \Lambda$, then we have that $\text{supp}(\mathbf{x}^*) = \Lambda$ and so it follows that $\mathbf{x}^* \succ 0$, i.e., the solution of the lasso is nonnegative. This implies that the solution of PL-NLasso for the same input and parameter value obeys $\hat{\mathbf{x}} = \mathbf{x}^*$ (i.e., the solution of the PL-NLasso problem matches the solution of the unconstrained lasso problem), and so $\text{supp}(\hat{\mathbf{x}}) = \text{supp}(\mathbf{x}^*) = \Lambda = \text{supp}(\mathbf{x}^{\text{true}})$. \square

The sufficient condition is composed of two inequalities; the first one (8) explains how much deviation from linearity is allowed, and the second one (9) shows the minimum value of the coefficient to be detected. This condition is a demanding sufficient MRC as we showed in [31]. Therefore, there are still many observations on which the PL-NLasso is successful, but for which the condition is not met.

3 MAIN RESULTS

3.1 Fundamental results for PL-NLasso

This section provides MRCs for which the subset of atoms Λ contains the support of minimizers of the PL-NLasso problem. In particular, we will give a condition for which a minimizer of the restricted PL-NLasso problem

$$\begin{aligned} & \underset{\mathbf{v}_\Lambda}{\text{minimize}} \quad \frac{1}{2} \|\mathbf{y} - \mathbf{A}_\Lambda \mathbf{v}_\Lambda\|_2^2 + \gamma \|\mathbf{v}_\Lambda\|_1 \\ & \text{subject to} \quad \mathbf{v}_\Lambda \succeq \mathbf{0}, \end{aligned} \quad (12)$$

also becomes a minimizer of the original problem (2). The condition is given by the following theorem.

Theorem 3.1. Let Λ be a subset of column indices of the dictionary matrix \mathbf{A} such that $|\Lambda| = J \leq N$. If the inequalities

$$(\mathbf{y} - \mathbf{A}_\Lambda \hat{\mathbf{v}}_\Lambda)^\top \mathbf{a}_j < \gamma \quad \text{for all } j \in \Lambda^c \quad (13)$$

hold for all solutions $\hat{\mathbf{v}}_\Lambda \in \mathbb{R}^J$ of the restricted PL-NLasso problem (12) over the column subset Λ , then all solutions to the general PL-NLasso (2) have their supports contained in Λ .

A proof of this theorem is found in the appendix. This theorem states a condition for which the restricted PL-NLasso problem (12) yields a global solution of the original problem (2). Although this condition requires the solutions of the restricted PL-NLasso problem, the theorem considers quite general cases:

- 1) the subdictionary \mathbf{A}_Λ can have linearly dependent columns,
- 2) the restricted PL-NLasso over columns in Λ can have multiple minimizers,

- 3) the entries of \mathbf{A} can be either positive or negative, or zero.

Thus, the theorem serves as a fundamental result to derive other practical MRCs in subsequent sections. When atoms associated with indices in Λ are linearly independent to each other, we can further assume the uniqueness of the solution because the restricted problem has the unique solution.

The condition (13) is a sufficient but not necessary condition for the event $\text{supp}(\hat{\mathbf{x}}) \subseteq \Lambda$. However, (13) is quite close to a necessary condition, as shown in the following theorem.

Theorem 3.2. Under the assumption of Theorem 3.1, if the support $\text{supp}(\hat{\mathbf{x}})$ of each solution $\hat{\mathbf{x}}$ to the general PL-NLasso (2) is contained in Λ , then the following condition holds for all solutions $\hat{\mathbf{v}}_\Lambda \in \mathbb{R}^J$ of the restricted PL-NLasso problem (12) over the column subset Λ :

$$(\mathbf{y} - \mathbf{A}_\Lambda \hat{\mathbf{v}}_\Lambda)^\top \mathbf{a}_j \leq \gamma \quad \text{for all } j \in \Lambda^c. \quad (14)$$

The proof of this theorem is found in the appendix. This theorem indicates that the condition (14) is a necessary condition for $\text{supp}(\hat{\mathbf{x}}) \subseteq \Lambda$. Hence a necessary and sufficient condition for the event $\text{supp}(\hat{\mathbf{x}}) \subseteq \Lambda$ lies somewhere between (13) and (14). More specifically, equalities need to be added to (13) only for some indices j to obtain a necessary and sufficient condition. Nonetheless, it is worth noting that the cases in which (14) holds with equality will be rare in practice. Therefore, the conditions (13) and (14) are practically identical, implying that (13) is a practically valid necessary and sufficient condition for the event $\text{supp}(\hat{\mathbf{x}}) \subseteq \Lambda$.

3.2 Approximately Perfect MRC for the PL-NLasso

This section provides MRCs for which the subset of atoms Λ becomes the exact support of minimizers of the PL-NLasso. We assume that atoms associated with indices in Λ are linearly independent. First, we define a metric that we call *positive subset coherence* (PSC) by

$$\text{PSC}(\Lambda; j) := 1 - \mathbf{1}_J^\top \mathbf{A}_\Lambda^\dagger \mathbf{a}_j. \quad (15)$$

The PSC is a metric to measure how positively aligned the j^{th} atom \mathbf{a}_j in the library is to the convex cone determined by the columns of \mathbf{A}_Λ . The index j is usually selected from outside Λ . The PSC becomes positive when the orthogonal projection of \mathbf{a}_j onto the orthogonal subspace spanned by the column vectors of \mathbf{A}_Λ falls on the opposite side from the origin about the hyperplane passing through the column vectors of \mathbf{A}_Λ ; negative when the origin and the column \mathbf{a}_j are on the same side of the aforementioned hyperplane; and zero when \mathbf{a}_j is contained in this hyperplane. This PSC plays an important role in the next approximately perfect MRC.

Theorem 3.3 (Approximately Perfect MRC for the PL-NLasso). Let Λ be a subset of column indices of the dictionary matrix \mathbf{A} such that $|\Lambda| = J \leq \min(L, N)$ and the atoms associated with indices in Λ are linearly independent. Let $\hat{\mathbf{x}}$ be a minimizer of the PL-NLasso

problem. The support of $\hat{\mathbf{x}}$, $\text{supp}(\hat{\mathbf{x}})$, is equal to Λ if the following two conditions hold:

- 1) Minimum coefficient condition (MCC):

$$\mathbf{A}_\Lambda^\dagger \mathbf{y} \succ \gamma (\mathbf{A}_\Lambda^\top \mathbf{A}_\Lambda)^{-1} \mathbf{1}_J \quad (16)$$

- 2) Non-linearity vs. Subset Coherence Condition (NSCC):

$$\mathbf{y}^\top \mathbf{P}_\Lambda^\perp \mathbf{a}_j < \gamma \text{PSC}(\Lambda; j) \quad \text{for all } j \in \Lambda^c. \quad (17)$$

Furthermore, the minimizer $\hat{\mathbf{x}}$ is equal to the appropriate zero-padding of the solution to the restricted PL-NLasso

$$\hat{\mathbf{v}}_\Lambda = \mathbf{A}_\Lambda^\dagger \mathbf{y} - \gamma (\mathbf{A}_\Lambda^\top \mathbf{A}_\Lambda)^{-1} \mathbf{1}_J.$$

The proof of this theorem is found in Section 3.3. The theorem has two conditions: MCC (16) and NSCC (17). The MCC measures whether the entries of the least squares solution ($\mathbf{A}_\Lambda^\dagger \mathbf{y}$) are sufficiently large. The NSCC specifies the nonlinearity magnitude that can be tolerated with respect to each PSC. The left hand side of (17) is the inner product between \mathbf{a}_j and the orthogonal projection of \mathbf{y} onto the orthogonal complement of $\mathcal{R}(\mathbf{A}_\Lambda)$. This quantity can be interpreted as a non-linearity because it is considered as the deviation from the span of \mathbf{A}_Λ . As explained, the right hand side of (17) quantifies the alignment of \mathbf{a}_j with the convex cone obtained from \mathbf{A}_Λ . Because γ is usually positive, a larger PSC relaxes the upper bound of $\mathbf{y}^\top \mathbf{P}_\Lambda^\perp \mathbf{a}_j$. Thus, it is preferable for \mathbf{a}_j to be less aligned to the columns of \mathbf{A}_Λ .

Interestingly, Conditions (8) and (9) in Theorem 2.2 are similar to the NSCC and MCC, but the former are not specific to particular indices j . This structure of the condition is shared with the simplified sufficient conditions derived in Section 3.4.

3.3 Proof of Theorem 3.3

Recall that the atoms associated with the index set Λ are linearly independent to each other and the two conditions (16) and (17) hold. First let us consider the restricted PL-NLasso problem defined by (12). The problem (12) has the unique minimizer because the objective function is strictly convex and the domain is a convex region. The Lagrangian of (12) is given by

$$L(\mathbf{v}_\Lambda, \boldsymbol{\lambda}) = \frac{1}{2} \|\mathbf{y} - \mathbf{A}_\Lambda \mathbf{v}_\Lambda\|_2^2 + \gamma \mathbf{1}_J^\top \mathbf{v}_\Lambda - \boldsymbol{\lambda}^\top \mathbf{v}_\Lambda,$$

where $\boldsymbol{\lambda} \in \mathbb{R}^J$ is a Lagrange multiplier with $\boldsymbol{\lambda} \succeq \mathbf{0}$. According to Theorem 28.3 [32, p. 281], if $\mathbf{v}_\Lambda = \hat{\mathbf{v}}_\Lambda$ and $\boldsymbol{\lambda} = \hat{\boldsymbol{\lambda}}$ satisfy the following conditions

- 1) $\hat{\mathbf{v}}_\Lambda, \hat{\boldsymbol{\lambda}} \succeq \mathbf{0}$ and $\hat{\boldsymbol{\lambda}}(n) \hat{\mathbf{v}}_\Lambda(n) = 0$ for all $n = 1, \dots, J$
- 2) $\mathbf{0} = \partial L(\mathbf{v}_\Lambda, \hat{\boldsymbol{\lambda}}) / \partial \mathbf{v}_\Lambda |_{\mathbf{v}_\Lambda = \hat{\mathbf{v}}_\Lambda}$.

Those conditions are true for $\hat{\mathbf{v}}_\Lambda = \mathbf{A}_\Lambda^\dagger \mathbf{y} - \gamma (\mathbf{A}_\Lambda^\top \mathbf{A}_\Lambda)^{-1} \mathbf{1}_J$ and $\hat{\boldsymbol{\lambda}} = \mathbf{0}$. Taking the uniqueness of the solution into consideration, we can conclude that the unique minimizer of (12) is given by

$$\hat{\mathbf{v}}_\Lambda = \mathbf{A}_\Lambda^\dagger \mathbf{y} - \gamma (\mathbf{A}_\Lambda^\top \mathbf{A}_\Lambda)^{-1} \mathbf{1}_J \succ \mathbf{0}. \quad (18)$$

By substituting (18) to the inequality (17), we have

$$\begin{aligned}
& (\mathbf{y} - \mathbf{A}_\Lambda \mathbf{A}_\Lambda^\dagger \mathbf{y})^\top \mathbf{a}_j < \gamma (1 - \mathbf{1}_J^\top \mathbf{A}_\Lambda^\dagger \mathbf{a}_j) \\
\Leftrightarrow & (\mathbf{y} - \mathbf{A}_\Lambda \mathbf{A}_\Lambda^\dagger \mathbf{y} + \gamma (\mathbf{A}_\Lambda^\dagger)^\top \mathbf{1}_J)^\top \mathbf{a}_j < \gamma \\
\Leftrightarrow & \{ \mathbf{y} - \mathbf{A}_\Lambda (\mathbf{A}_\Lambda^\dagger \mathbf{y} - \gamma (\mathbf{A}_\Lambda^\top \mathbf{A}_\Lambda)^{-1} \mathbf{1}_J) \}^\top \mathbf{a}_j < \gamma \\
\Leftrightarrow & (\mathbf{y} - \mathbf{A}_\Lambda \hat{\mathbf{v}}_\Lambda)^\top \mathbf{a}_j < \gamma \quad (\because (18))
\end{aligned}$$

for all $j \in \Lambda^c$. Directly applying Theorem 3.1, we can assert that Λ contains the support of $\hat{\mathbf{x}}$. Furthermore, since all the elements of the minimizer (18) are greater than zero, Λ is the support of $\hat{\mathbf{x}}$. This completes the proof. \blacksquare

3.4 Simplified sufficient conditions for PL-NLasso

Although these conditions are quite simple, they are still more elaborate than those provided by Tropp [30] for general lasso. We will further simplify and introduce two sufficient conditions in this section. To start with, we define the positive exact recovery coefficient (PERC) by

$$\text{PERC}(\Lambda) := \min_{j \in \Lambda^c} \text{PSC}(\Lambda; j).$$

We call this PERC because this is considered as the positive counterpart of the ERC, and PERC is interpreted as the minimum of the right hand side in the NSCC (17). We can also take the maximum on the left hand side of the inequality (17) after concatenating all \mathbf{a}_j , and then a modified sufficient condition for the multiple NSCCs is written as

$$\max_{j \in \Lambda^c} \mathbf{a}_j^\top \mathbf{P}_\Lambda^\perp \mathbf{y} < \gamma \text{PERC}(\Lambda). \quad (19)$$

We refer to this condition (19) as PERC-Max condition. Using this, we can derive a next corollary.

Corollary 3.4 (PERC Max MRC for PL-NLasso). Under the assumptions of Theorem 3.3, the support of $\hat{\mathbf{x}}$, $\text{supp}(\hat{\mathbf{x}})$, is equal to Λ if the two conditions, MCC (16) and PERC-Max (19) condition, hold. Furthermore, the minimizer $\hat{\mathbf{x}}$ is also given as in Theorem 3.3.

We can still introduce another NSCC condition that is more strict than Corollary 3.4 but more relaxed than Theorem 2.2 by taking the absolute maximum value on the left side of (19),

$$\|\mathbf{A}^\top \mathbf{P}_\Lambda^\perp \mathbf{y}\|_\infty < \gamma \text{PERC}(\Lambda), \quad (20)$$

We refer this condition as PERC-absolute Max (PERC-AMax) condition, leading to the next corollary.

Corollary 3.5 (PERC-absolute Max MRC for PL-NLasso). Under the assumptions of Theorem 3.3, the support of $\hat{\mathbf{x}}$, $\text{supp}(\hat{\mathbf{x}})$, is equal to Λ if the two conditions, MCC (16) and PERC-AMax (20) condition, hold. Furthermore, the minimizer $\hat{\mathbf{x}}$ is also given as in Theorem 3.3.

The PERC-AMax condition is more demanding than the PERC-Max condition. Additionally, it provides a broader guarantee than Theorem 2.2, which assumes the linear model (1) and requires not only the support of the true coefficient vector \mathbf{x}^{true} but also its values and the error term in advance, while Corollary 3.5 can be applied to arbitrary vectors \mathbf{y} and index sets Λ .

4 APPLICATION TO HYPERSPECTRAL UNMIXING

Hyperspectral imagers collect electromagnetic radiation over the Visible and Near Infrared (VNIR) to Short Wave Infrared (SWIR) region (300-2600nm) with hundreds of narrow contiguous bands. Each pixel position of a hyperspectral image (HSI) is associated with a *spectrum* or *spectral signature*, an array of dimension equal to the number of bands, which is used by practitioners to reveal the compositional characteristics of targets in a variety of applications.

One of the tasks routinely performed in hyperspectral imaging is spectral unmixing. Unmixing is a process to decompose an observed spectrum into pure constituent signatures, which are usually called *endmembers*, associated with their fractional abundances [33], [34]. The linear model (1) has been widely used in unmixing, where \mathbf{y} represents the observed spectrum, \mathbf{A} is the dictionary matrix with atoms corresponding to endmember spectra, and the coefficient vector \mathbf{x} is interpreted as a fractional abundance vector.

Recently, sparse unmixing [10] has been proposed for hyperspectral unmixing tasks where one is given a large collection — the *spectral library* — of pure spectral signatures to be used as candidate endmembers. The first goal for unmixing is to correctly identify the library spectra that are combined to form the observed spectrum. One typically expects that only a few endmembers in the collection are involved in the observation, as the number of materials occupying the region subtended by a pixel is small in most scenarios. Motivated by this observation, sparse unmixing [10] employs PL-NLasso to detect endmembers and estimate abundances for hyperspectral images using a large library of laboratory spectra.

Nonetheless, sparse unmixing faces several limitations in practical applications. An observed spectrum could be composed by a *non-linear* mixture of endmembers. The atoms in the library might not match exactly the image endmembers (typical examples are spectra of the same material acquired at different conditions). Moreover, the library spectra are usually highly correlated, which intuitively seems undesirable for the non-negative sparse modeling.

Given such complications, we propose the theorems derived in this paper as a way to assess the performance of PL-NLasso in hyperspectral unmixing. Since we have not restricted the definition of the “error” term e in the linear model equation (1), it could accommodate any deviation from linearity, such as non-linear mixing or spectral distortions.

We test the performance of PL-NLasso in unmixing a real hyperspectral image of an oil painting. In particular, we are interested in assessing the performance of the sparse modeling approach in identifying the endmembers involved in each pixel of the HSI. This example presents the typical complications of unmixing problems: the artist creates the colors in the painting by mechanically mixing the paints (non-linear mixing) and adding water (non-linear distortion of all pixel spectra). Further non-linearities stem from the different density and thickness of the paint in different regions. We first describe the creation of training data including endmembers and their true abundance maps. We then assess the ability of the MRCs to predict the outcome of numerical computations using PL-NLasso.

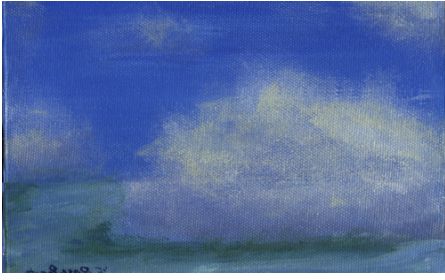


Fig. 1. 500×308 pseudo RGB color image of a hyperspectral image of the oil painting. R: band 125 (601nm), G: band 86 (536nm), B: band 49 (471nm).

4.1 Data set

The data set used for this experiment is a hyperspectral image (HSI) of an oil painting acquired by a Micro-Hyperspec[®] VNIR imaging sensor (E-Series).¹ The imager captures spectral information in the 400-1000nm wavelength region with 370 bands at 1.6nm intervals. The image was acquired on Hyperspec Starter Kit manufactured by Headwall Inc. Since the painting was larger than the field of view of the camera we first separated the whole area into three strip regions, acquired the images of them separately, and stitched them together. The size of the resulting hyperspectral image is $3347 \times 1233 \times 370$, where the first two dimensions are the number of pixels in the spatial directions and the last dimension records the number of spectral bands. The image was converted to reflectance using a Spectralon[®] reference.² The image was then spatially downsampled to 500×308 by a 4×4 averaging filter in order to improve its signal-to-noise ratio. Figure 1 shows a pseudo RGB rendition of the HSI.

The artist used acrylic paint in five distinct colors: red, blue, yellow, white, and green. We acquired an HSI of the pure colors, which is shown on the lower left side in Figure 2. The averaged spectra of the five colored areas can be considered as the endmembers of the pixels depicting the painting and are also shown in Figure 2.

The artist did not provide in advance the information about true distribution of the endmembers for each pixel. We will use the term ‘‘ground truth’’, borrowed from hyperspectral remote sensing, for such map. This information is required in order to assess the performance of the unmixing algorithm. Since the artist used 2 or 3 colors at each location (single-endmember pixels are not present) we could generate the ground truth by solving the following minimization problem for each pixel

$$\begin{aligned} & \underset{\mathbf{x}}{\text{minimize}} && \frac{1}{2} \|\mathbf{y} - \mathbf{A}\mathbf{x}\|_2^2 \\ & \text{subject to} && \mathbf{x} \geq \mathbf{0}, \|\mathbf{x}\|_0 \leq 3. \end{aligned} \quad (21)$$

In practice, we found the solution by conducting least square minimizations for all possible combinations of 2 or 3 endmembers and we selected as the ground truth the combination with the smallest number of endmembers among the ones that achieved the least error. Figure 3 shows the ground

1. Micro-Hyperspec[®] is a registered trademark of Headwall Photonics, Inc.

2. Spectralon[®] is a registered trademark of Labsphere, Inc.

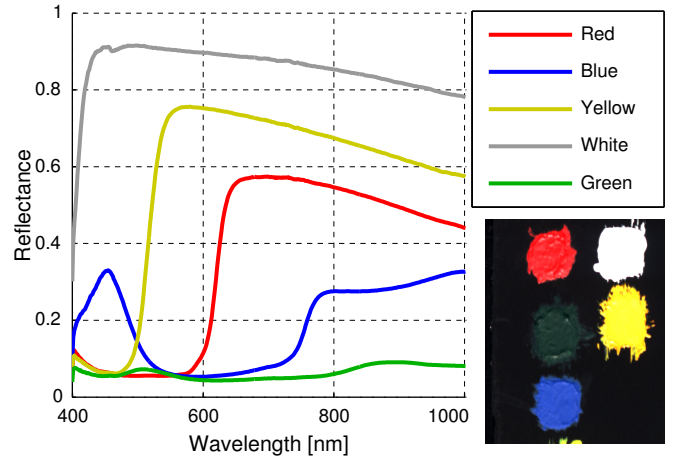


Fig. 2. Averaged endmember spectra. The image on the lower left is a pseudo RGB color image of a hyperspectral image of endmembers.

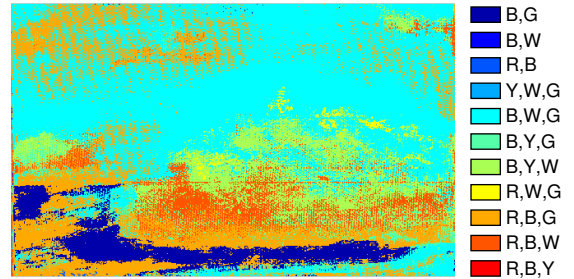


Fig. 3. The true distribution of the mixtures. The letters R, B, Y, W, and G are the first letters of the pure colors.

truth at each pixel. We note that although the minimization problem above also produces abundance values for each endmember at each pixel location, we are discarding such information as we are interested in endmember retrieval performance. Furthermore, while we were able to confirm with the artist that the retrieved distribution is accurate, a similar assessment would not be possible for the abundances. We nevertheless report the abundances for all colors in Figure 4 for the sake of completeness and to show that they show reasonable effects. From Figure 4, one can see that the white color is dominant around the clouds in Figure 1, the sky is mainly painted in white and blue, and the grass that can be found around the bottom in Figure 1 consists of mainly green.

4.2 Theorem validation

In this section, we evaluate the predictive power of the MRCs. The performance of the PL-NLasso is predicted by four MRCs: Theorem 2.2 (ERC-based MRC), Theorem 3.3 (APMRC), Corollary 3.4 (PERC-Max MRC), and Corollary 3.5 (PERC-AMax MRC). The algorithm we employed to produce numerical solutions the PL-NLasso is the sparse unmixing by variable splitting and augmented Lagrangian (SUNSAL) [35]. We are interested in determining how well the predictions of the MRCs match the result obtained by SUNSAL.

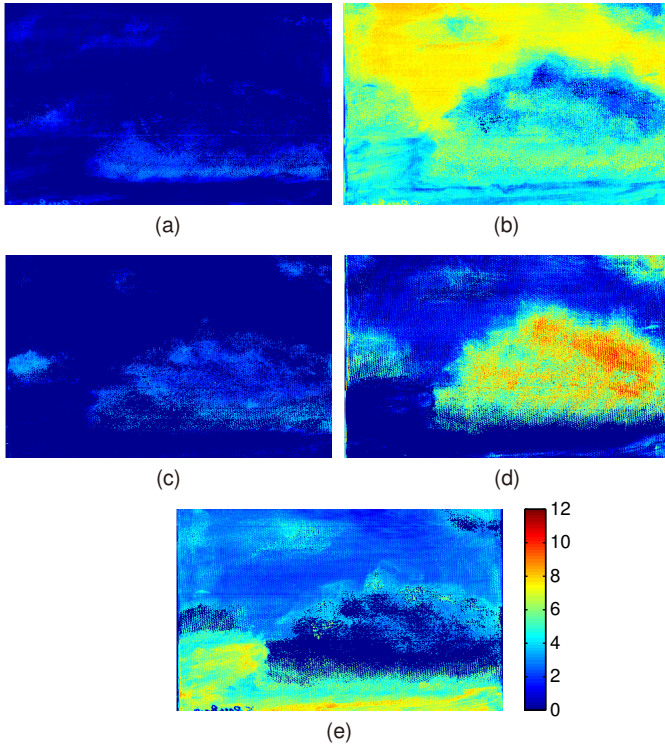


Fig. 4. The true abundance maps in the painting image: (a) red, (b) blue, (c) yellow, (d) white, and (e) green.

Table 1 shows the number of pixels that satisfy each of MRCs hold for a different value of $\gamma = 0.2, 0.1, 0.05$. For each value of γ we display the confusion matrix between the prediction by each MRC and the SUnSAL result. In each row, the label “True” refers to the points fulfilling the specific condition and “False” the ones violating it. Similarly, in each column, the label “Correct” (“Incorrect”) refers to points for which SUnSAL correctly identifies (fails to identify) the endmembers.

For all the MRCs, the values in the True-Incorrect cells are all zeros, indicating that if the MRCs hold, the SUnSAL always succeeds. This is a confirmation for the sufficiency of all the MRCs in all the theorems.

One remarkable fact is that the “False-Correct” cell of the APMRC is always zero, which means the APMRC is always true when SUnSAL succeeds in detecting the correct endmembers, confirming the necessity of the APMRC condition in practical settings. In contrast, there are non-zero values in the False-Correct cells for the other MRCs, and the values increase as the conditions become increasingly strict.

None of the pixels satisfy the strict conditions required by the ERC-based MRC. It is worth noting that the application we chose tests the limits of the theory of sparse recovery in at least two ways. First, hyperspectral mixing processes can deviate significantly from the linear model; second, spectra of different endmembers are very correlated. In our view, this observation supports the utility of the APMRC, PERC-Max MRC and PERC-AMax MRC as prediction tools for signal spaces in which previously proposed metrics would not be applicable.

Figure 5 shows an interesting behavior in the perfor-

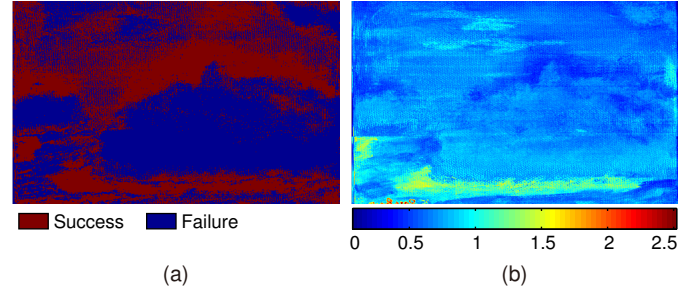


Fig. 5. (a) The distribution of correct model recovery of the PL-NLasso and (b) The distribution of the deviation from the linear model.

mance of the PL-NLasso. In Figure 5(a), the pixels where the PL-NLasso succeeds at identifying endmembers are shown in red, while failures are shown in blue. Figure 5(b) shows the distribution of the residual given by the optimum value of (21). This residual is interpreted as the deviation from linearity; therefore, one may expect that a large deviation is linked to failure of the PL-NLasso, but this intuition does not bear out in practice. Deviations seem to be relatively high in the horizontal belt near the bottom of the painting, but the PL-NLasso is able to detect the correct endmembers in that area. The reason for this phenomenon is explained in Figure 6. In this figure, we focus only on the region classified as the mixture of blue and green that mostly overlaps with the horizontally belted region. Figures 6(a,c,e) shows the distribution of the values $\mathbf{y}^T \mathbf{P}_\Lambda^\perp \mathbf{a}_j$ and Figures 6(b,d,f) shows the distribution of the values $\text{PSC}(\Lambda; j)$ Where j indexes the red, yellow, and white colors. The values in the region of interest in Figures 6(a,c,e) are always negative, while those in Figures 6(b,d,f) are always positive, meaning the NSCC conditions for the APMRC, PERC-Max MRC, PERC-AMax MRC are always true. Even when the deviation is large, the PL-NLasso might be successful if the residual is negatively correlated with the signatures of all the other endmembers and PSC is positive and vice versa. Although this does not always happen, but this specific example demonstrates that the direction of the deviation affects the performance of the PL-NLasso.

One final observation about Figure 5(b) is that the region of maximum deviation from nonlinearity (green to yellow) corresponds with a region to which the artist confirmed having applied more than one layer of paint (this is called *pentimento* in art jargon). This is consistent with our understanding of the radiative transfer aspects of unmixing, e.g [34] and suggests the potential utility of unmixing techniques to aspects of the artist painting style in addition to identifying the different pigments.

5 CONCLUSION

In this paper, we explored several recovery conditions that guarantee the correct identification of endmembers by the non-negative sparse modeling for mixed signals exhibiting deviations from linearity. Those conditions reveal an interesting property of the PL-NLasso, which is expressed by two conditions: minimum coefficient condition and non-linearity vs subset coherence condition. In particular, we derived an almost perfect condition that can exactly predict

TABLE 1
Performance of MRCs on the painting data

		$\gamma = 0.2$		$\gamma = 0.1$		$\gamma = 0.05$	
		SUnSAL retrieval		SUnSAL retrieval		SUnSAL retrieval	
		Correct	Incorrect	Correct	Incorrect	Correct	Incorrect
Thm. 3.3 (APMRC)	True	56718 [pts]	0	70256	0	64459	0
	False	0	97282	0	83744	0	89541
Cor. 3.4 (PERC-Max MRC)	True	56053	0	67252	0	62547	0
	False	665	97282	3004	83744	1912	89541
Cor. 3.5 (PERC-AMax MRC)	True	46349	0	53122	0	32361	0
	False	10369	97282	17134	83744	32098	89541
Thm. 2.2 (ERC-based MRC)	True	0	0	0	0	0	0
	False	56718	97282	70256	83744	64459	89541

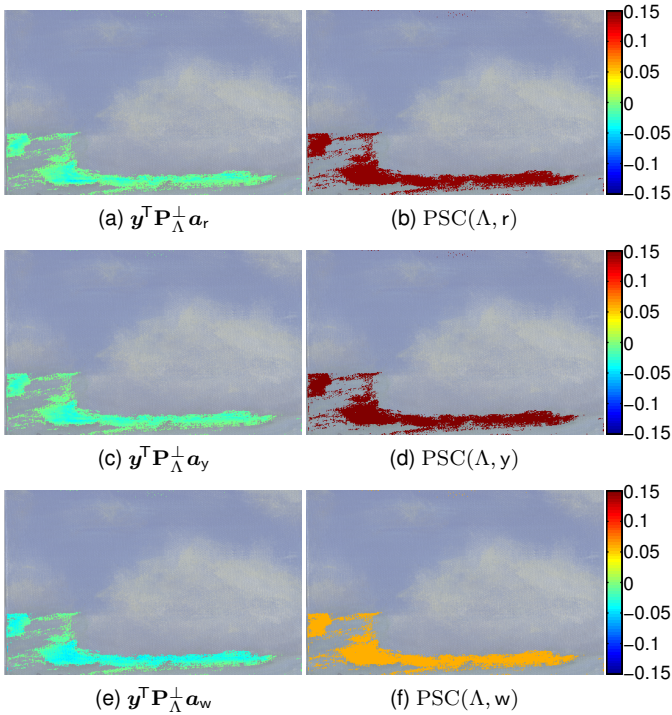


Fig. 6. Comparison of the left hand side and right hand side of the NSCC. The letters, r, y, and w, means the first letter of the three colors: red, yellow, and white.

the performance of the PL-NLasso in a practical sense. The exactness was inferred from mathematical inspection and further verified through experiments. These conditions are proven to be useful for analyzing the performance of numerical solutions of the PL-NLasso.

APPENDIX PROOF OF THEOREMS 3.1 AND 3.2

In this appendix, we prove Theorems 3.1 and 3.2 together because they share assumptions. Recall the PL-NLasso:

$$\begin{aligned} & \underset{\mathbf{x}}{\text{minimize}} && \frac{1}{2} \|\mathbf{y} - \mathbf{A}\mathbf{x}\|_2^2 + \gamma \mathbf{1}_N^\top \mathbf{x} \\ & \text{subject to} && \mathbf{x} \succeq \mathbf{0} \end{aligned}$$

where $\mathbf{A} \in \mathbb{R}^{L \times N}$ is a dictionary matrix and the $\mathbf{y} \in \mathbb{R}^L$ is an observation signal. We prove the next two statements:

$$\text{(Theorem 3.1)} \quad (13) \Rightarrow \text{supp}(\hat{\mathbf{x}}) \subseteq \Lambda \quad (22)$$

$$\text{(Theorem 3.2)} \quad \text{supp}(\hat{\mathbf{x}}) \subseteq \Lambda \Rightarrow (14) \quad (23)$$

where $\hat{\mathbf{x}}$ is a minimizer of the PL-NLasso.

Before proceeding with the proof, we first transform the event $\text{supp}(\hat{\mathbf{x}}) \subseteq \Lambda$ into an equivalent form. More specifically, $\text{supp}(\hat{\mathbf{x}}) \subseteq \Lambda$ means that the solution of the PL-NLasso is equivalent to a solution of the restricted problem (12), $\hat{\mathbf{v}}_\Lambda$, with appropriate zero-padding; this can be written as $\mathbf{A}\hat{\mathbf{x}} = \mathbf{A}_\Lambda \hat{\mathbf{v}}_\Lambda$, where $\hat{\mathbf{v}}_\Lambda$ is an optimal solution of the restricted PL-NLasso problem. We rewrite the problem as

$$\begin{aligned} & \underset{\mathbf{v}_\Lambda}{\text{minimize}} && \frac{1}{2} \|\mathbf{y} - \mathbf{A}_\Lambda \mathbf{v}_\Lambda\|_2^2 + \gamma \mathbf{1}_J^\top \mathbf{v}_\Lambda \\ & \text{subject to} && \mathbf{v}_\Lambda \succeq \mathbf{0}. \end{aligned} \quad (24)$$

Thus, we have $\text{supp}(\hat{\mathbf{x}}) \subseteq \Lambda$ if and only if the following inequality holds:

$$\frac{1}{2} \|\mathbf{y} - \mathbf{A}\hat{\mathbf{x}}\|_2^2 + \gamma \mathbf{1}_N^\top \hat{\mathbf{x}} < \frac{1}{2} \|\mathbf{y} - \mathbf{A}(\hat{\mathbf{x}} + \Delta\mathbf{x})\|_2^2 + \gamma \mathbf{1}_N^\top (\hat{\mathbf{x}} + \Delta\mathbf{x}) \quad (25)$$

for every $\Delta\mathbf{x}$ such that $0 < \Delta x_j$ for any $j \in \Lambda^c$ and $\mathbf{x} + \Delta\mathbf{x} \succeq \mathbf{0}$ where Δx_j is the j^{th} element of \mathbf{x} . In other words, the minimum cost achieved by the solution of the restricted problem is less than any cost achieved by another \mathbf{x} that involves an atom outside Λ . Let the exact support of $\hat{\mathbf{x}}_\Lambda$ be $\Gamma \subseteq \Lambda$ ($|\Gamma| = M \leq J$). Then the inequality $\mathbf{x} + \Delta\mathbf{x} \succeq \mathbf{0}$ is expressed as:

$$\begin{aligned} & 1) \quad -x_j \leq \Delta x_j \text{ for all } j \in \Gamma \\ & 2) \quad 0 \leq \Delta x_j \text{ for all } j \in \Gamma^c, \end{aligned} \quad (26)$$

which defines a region of interest for the vector $\Delta\mathbf{x}$. By canceling terms common to both sides, the inequality (25) is transformed into

$$\begin{aligned} & \frac{1}{2} \|\mathbf{A}(\Delta\mathbf{x})\|_2^2 + \gamma \mathbf{1}_N^\top (\Delta\mathbf{x}) - (\mathbf{y} - \mathbf{A}_\Lambda \hat{\mathbf{v}}_\Lambda)^\top \mathbf{A}(\Delta\mathbf{x}) > 0 \\ \Leftrightarrow & \frac{1}{2} \|\mathbf{A}(\Delta\mathbf{x})\|_2^2 + \sum_{j \in \Omega} \Delta x_j (\gamma - \mathbf{a}_j^\top (\mathbf{y} - \mathbf{A}_\Lambda \hat{\mathbf{v}}_\Lambda)) > 0. \end{aligned} \quad (27)$$

Next we explore a property of $\hat{\mathbf{v}}_\Lambda$. The Lagrangian of the restricted PL-NLasso (24) above is given by

$$L_\Lambda(\mathbf{v}_\Lambda, \boldsymbol{\lambda}_\Lambda) = \frac{1}{2} \|\mathbf{y} - \mathbf{A}_\Lambda \mathbf{v}_\Lambda\|_2^2 + \gamma \mathbf{1}_J^\top \mathbf{v}_\Lambda - \boldsymbol{\lambda}_\Lambda^\top \mathbf{v}_\Lambda,$$

where $\boldsymbol{\lambda}_\Lambda$ is a vector of Lagrangian multipliers. From the KKT condition in Theorem 28.3 [32, p. 281], $\mathbf{v}_\Lambda = \hat{\mathbf{v}}_\Lambda$ and $\boldsymbol{\lambda} = \hat{\boldsymbol{\lambda}}$ become a minimizer and a Kuhn-Tucker vector, respectively, if and only if the following three conditions hold:

$$1) \quad \hat{\mathbf{v}}_\Lambda, \hat{\boldsymbol{\lambda}}_\Lambda \succeq \mathbf{0} \quad (28a)$$

$$2) \quad \hat{\boldsymbol{\lambda}}_\Lambda(n) \hat{\mathbf{v}}_\Lambda(n) = 0 \text{ for all } n \quad (28b)$$

$$3) \quad \mathbf{0} = \partial L_\Lambda(\hat{\mathbf{v}}_\Lambda, \hat{\boldsymbol{\lambda}}_\Lambda) / \partial \mathbf{v}_\Lambda|_{\mathbf{v}_\Lambda = \hat{\mathbf{v}}_\Lambda}. \quad (28c)$$

The third KKT condition (28c) is equivalently expressed as:

$$\begin{aligned} & \mathbf{A}_\Lambda^\top (\mathbf{A}_\Lambda \hat{\mathbf{v}}_\Lambda - \mathbf{y}) + \gamma \mathbf{1}_J - \hat{\boldsymbol{\lambda}}_\Lambda = \mathbf{0} \\ \Leftrightarrow & \gamma - \mathbf{a}_j^\top (\mathbf{y} - \mathbf{A}_\Lambda \hat{\mathbf{v}}_\Lambda) = \hat{\boldsymbol{\lambda}}_\Lambda(j) \quad \text{for all } j \in \Lambda \end{aligned}$$

For $j \in \Gamma$, we have $\hat{\mathbf{v}}_\Lambda(j) > 0$, leading to $\hat{\boldsymbol{\lambda}}_\Lambda(j) = 0$ because of the second KKT condition (28b). For $j \in \Lambda \setminus \Gamma$, we have $\hat{\mathbf{v}}_\Lambda(j) = 0$, leading to $\hat{\boldsymbol{\lambda}}_\Lambda(j) \geq 0$. Thus we have

$$\begin{cases} \gamma - \mathbf{a}_j^\top (\mathbf{y} - \mathbf{A}_\Lambda \hat{\mathbf{v}}_\Lambda) = 0 \text{ for } j \in \Gamma \\ \gamma - \mathbf{a}_j^\top (\mathbf{y} - \mathbf{A}_\Lambda \hat{\mathbf{v}}_\Lambda) \geq 0 \text{ for } j \in \Lambda \setminus \Gamma. \end{cases} \quad (29)$$

Considering the conditions above for $\hat{\mathbf{v}}_\Lambda$, the inequality (27) is equivalently transformed into

$$\begin{aligned} & \frac{1}{2} \|\mathbf{A}(\Delta \mathbf{x})\|_2^2 + \sum_{j \in \Lambda \setminus \Gamma} \Delta x_j (\gamma - \mathbf{a}_j^\top (\mathbf{y} - \mathbf{A}_\Lambda \hat{\mathbf{v}}_\Lambda)) \\ & + \sum_{j \in \Lambda^c} \Delta x_j (\gamma - \mathbf{a}_j^\top (\mathbf{y} - \mathbf{A}_\Lambda \hat{\mathbf{v}}_\Lambda)) > 0, \end{aligned} \quad (30)$$

where the second term is always non-negative because of the non-negativity of the two factors ((26) and (29)). Summarizing this discussion, $\text{supp}(\hat{\mathbf{x}}) \subseteq \Lambda$ if and only if the inequality (30) holds for all $\Delta \mathbf{x}$ in the defined region (26).

We now prove the statement (22) for Theorem 3.1. Given the condition (13) is true, then the summation of the third term on the left side in (30) becomes always non-negative. Furthermore, because we are considering $\Delta \mathbf{x}$ with a non-zero j^{th} element for any $j \in \Lambda^c$, the third term is always strictly positive. Therefore, (30) holds for every $\Delta \mathbf{x}$ in the defined region. Because that condition is equivalent to $\text{supp}(\hat{\mathbf{x}}) \subseteq \Lambda$, the statement (22) is proven.

Next, we prove the statement (23) for Theorem 3.2. We prove this by the principle of contradiction. Assume the inequality (30) is true for every $\Delta \mathbf{x}$ in the defined region and every solution $\hat{\mathbf{v}}_\Lambda$. Suppose there exists a solution $\hat{\mathbf{v}}_\Lambda$ and an index $j' \in \Lambda^c$ such that

$$(\mathbf{y} - \mathbf{A}_\Lambda \hat{\mathbf{v}}_\Lambda)^\top \mathbf{a}_{j'} > \gamma$$

The inequality (30) is true for $\Delta \mathbf{x}'$ such that only the j^{th} element is greater than zero and the others are zero. Let such a $\Delta \mathbf{x}'$ be

$$\Delta \mathbf{x}' = [0 \dots 0 \Delta x_{j'}, 0 \dots 0]^\top \quad (\Delta x_{j'} > 0), \quad (31)$$

then the inequality (30) becomes,

$$\frac{1}{2} \|\mathbf{a}_{j'}\|_2^2 (\Delta x_{j'})^2 - ((\mathbf{y} - \mathbf{A}_\Lambda \hat{\mathbf{v}}_\Lambda)^\top \mathbf{a}_{j'} - \gamma) \Delta x_{j'} > 0. \quad (32)$$

The left hand side is a quadratic function with regard to a scalar variable $\Delta x_{j'}$. Let both coefficients be

$$b_{j'} = \frac{1}{2} \|\mathbf{a}_{j'}\|_2^2 > 0 \quad (33)$$

$$c_{j'} = (\mathbf{y} - \mathbf{A}_\Lambda \hat{\mathbf{v}}_\Lambda)^\top \mathbf{a}_{j'} - \gamma > 0, \quad (34)$$

then the inequality is written as

$$\Delta x_{j'} (b_{j'} \Delta x_{j'} - c_{j'}) > 0. \quad (35)$$

Because both the coefficients $b_{j'}$ and $c_{j'}$ are positive, the left hand side becomes negative for sufficiently small $\Delta x_{j'}$ such that $0 < \Delta x_{j'} < c_{j'}/b_{j'}$. Since $\Delta x_{j'}$ can take any positive value, we can say that there exists a $\Delta x_{j'}$ that breaks the inequality (30). This contradicts to our starting assumption. Thus, by the principle of contradiction, the statement (23) is proven.

This completes the proof. \square

ACKNOWLEDGMENTS

This work was supported in part by the National Science Foundation under grant number IIS-1319585. We thank Rose Kontak for providing us with the oil painting, and José Bioucas-Dias for making Matlab code for SUNSAL available online.

REFERENCES

- [1] D. L. Donoho, "Compressed sensing," *IEEE Trans. Inf. Theory*, vol. 52, no. 4, pp. 1289–1306, Apr. 2006.
- [2] E. J. Candès, "The restricted isometry property and its implications for compressed sensing," *Comptes Rendus Math.*, vol. 346, no. 9710, pp. 589–592, May 2008.
- [3] D. D. Lee and H. S. Seung, "Learning the parts of objects by non-negative matrix factorization." *Nature*, vol. 401, no. 6755, pp. 788–91, Oct. 1999.
- [4] D. Heinz and C.-I. Chang, "Fully constrained least squares linear spectral mixture analysis method for material quantification in hyperspectral imagery," *IEEE Trans. Geosci. Remote Sens.*, vol. 39, no. 3, pp. 529–545, Mar. 2001.
- [5] M. D. Plumbley, "Algorithms for nonnegative independent component analysis," *IEEE Trans. Neural Networks*, vol. 14, no. 3, pp. 534–543, May 2003.
- [6] Y. Ji, T. Lin, and H. Zha, "Mahalanobis distance based Non-negative sparse representation for face recognition," in *Proc. Int. Conf. Mach. Learn. Appl.*, Miami Beach, FL, Dec. 2009, pp. 41–46.
- [7] R. He, W.-S. Zheng, B.-G. Hu, and X.-W. Kong, "Two-stage nonnegative sparse representation for large-scale face recognition," *IEEE Trans. Neural Networks Learn. Syst.*, vol. 24, no. 1, pp. 35–46, Jan. 2013.
- [8] J. Wright, A. Yang, A. Ganesh, S. Sastry, and Y. Ma, "Robust Face Recognition via Sparse Representation," *IEEE Trans. Pattern Anal. Mach. Intell.*, vol. 31, no. 2, pp. 210–227, Feb. 2009.
- [9] A. Szlam, Z. Guo, and S. Osher, "A split Bregman method for non-negative sparsity penalized least squares with applications to hyperspectral demixing," in *Proc. Int. Conf. Image Process.*, Hong Kong, Sep. 2010, pp. 1917–1920.
- [10] M.-D. Iordache, J. Bioucas-Dias, and A. Plaza, "Sparse unmixing of hyperspectral data," *IEEE Trans. Geosci. Remote Sens.*, vol. 49, no. 6, pp. 2014–2039, June 2011.
- [11] J. Bardsley and J. Nagy, "Covariance-preconditioned iterative methods for nonnegatively constrained astronomical imaging," *SIAM J. Matrix Anal. Appl.*, vol. 27, no. 4, pp. 1184–1197, Jan. 2006.
- [12] M. Slawski and M. Hein, "Sparse recovery for protein mass spectrometry data," in *Pract. Appl. Sparse Model.*, A. N.-M. I. Rish, G. Cecchi, A. Lozano, Ed. MIT Press, 2010.
- [13] D. L. Donoho and J. Tanner, "Sparse nonnegative solution of underdetermined linear equations by linear programming," *Proc. Natl. Acad. Sci.*, vol. 102, no. 27, pp. 9446–9451, July 2005.

- [14] —, “Neighborliness of randomly projected simplices in high dimensions,” *Proc. Natl. Acad. Sci. U. S. A.*, vol. 102, no. 27, pp. 9452–9457, July 2005.
- [15] D. Donoho and J. Tanner, “Thresholds for the recovery of sparse solutions via L1 minimization,” in *40th Annu. Conf. Inf. Sci. Syst.*, Princeton, NJ, Mar. 2006, pp. 202–206.
- [16] A. Bruckstein, M. Elad, and M. Zibulevsky, “On the uniqueness of nonnegative sparse solutions to underdetermined systems of equations,” *IEEE Trans. Inf. Theory*, vol. 54, no. 11, pp. 4813–4820, Nov. 2008.
- [17] M. Wang and A. Tang, “Conditions for a unique non-negative solution to an underdetermined system,” in *47th Annu. Allert. Conf. Commun. Control Comput.*, Sep. 2009, pp. 301–307.
- [18] M. Wang, W. Xu, and A. Tang, “A unique “nonnegative” solution to an underdetermined system: from vectors to matrices,” *IEEE Trans. Signal Process.*, vol. 59, no. 3, pp. 1007–1016, Mar. 2011.
- [19] M. Khajehnejad, A. Dimakis, W. Xu, and B. Hassibi, “Sparse recovery of nonnegative signals with minimal expansion,” *IEEE Trans. Signal Process.*, vol. 59, no. 1, pp. 196–208, Jan. 2011.
- [20] Y.-B. Zhao, “Equivalence and strong equivalence between the sparsest and Least ℓ_1 -norm nonnegative solutions of linear systems and their applications,” *J. Oper. Res. Soc. China*, vol. 2, no. 2, pp. 171–193, May 2014.
- [21] R. Tibshirani, “Regression shrinkage and selection via the lasso,” *J. R. Stat. Soc. Ser. B*, vol. 58, no. 1, pp. 267–288, Jan. 1996.
- [22] M. Wainwright, “Sharp thresholds for high-dimensional and noisy sparsity recovery using ℓ_1 -constrained quadratic programming (lasso),” *IEEE Trans. Inf. Theory*, vol. 55, no. 5, pp. 2183–2202, May 2009.
- [23] D. L. Donoho and M. Elad, “Optimally sparse representation in general (nonorthogonal) dictionaries via ℓ^1 minimization,” *Proc. Natl. Acad. Sci.*, vol. 100, no. 5, pp. 2197–2202, Mar. 2003.
- [24] P. Zhao and B. Yu, “On model selection consistency of lasso,” *J. Mach. Learn. Res.*, vol. 7, pp. 2541–2563, Nov. 2006.
- [25] P. J. Bickel, Y. Ritov, and A. B. Tsybakov, “Simultaneous analysis of Lasso and Dantzig selector,” *Ann. Stat.*, vol. 37, no. 4, pp. 1705–1732, Aug. 2009.
- [26] A. Cohen, W. Dahmen, and R. DeVore, “Compressed sensing and best k -term approximation,” *J. Am. Math. Soc.*, vol. 22, no. 1, pp. 211–231, 2009.
- [27] D. Donoho, M. Elad, and V. Temlyakov, “Stable recovery of sparse overcomplete representations in the presence of noise,” *IEEE Trans. Inf. Theory*, vol. 52, no. 1, pp. 6–18, Jan. 2006.
- [28] J. Fuchs, “Recovery of exact sparse representations in the presence of bounded noise,” *IEEE Trans. Inf. Theory*, vol. 51, no. 10, pp. 3601–3608, Oct. 2005.
- [29] J. Tropp, “Greed is good: algorithmic results for sparse approximation,” *IEEE Trans. Inf. Theory*, vol. 50, no. 10, pp. 2231–2242, Oct. 2004.
- [30] —, “Just relax: Convex programming methods for identifying sparse signals in noise,” *IEEE Trans. Inf. Theory*, vol. 52, no. 3, pp. 1030–1051, Mar. 2006.
- [31] Y. Itoh, M. F. Duarte, and M. Parente, “Performance guarantees for sparse regression-based unmixing,” in *IEEE GRS Work. Hyperspectral Image Signal Process. Evol. Remote Sens. (WHISPERS)*, Tokyo, Japan, June 2015.
- [32] R. T. Rockafellar, *Convex Analysis*. Princeton Univ. Press, 1970.
- [33] J. Bioucas-Dias, A. Plaza, N. Dobigeon, M. Parente, Q. Du, P. Gader, and J. Chanussot, “Hyperspectral Unmixing Overview: Geometrical, Statistical, and Sparse Regression-Based Approaches,” *IEEE J. Sel. Top. Appl. Earth Obs. Remote Sens.*, vol. 5, no. 2, pp. 354–379, Apr. 2012.
- [34] R. Heylen, M. Parente, and P. Gader, “A Review of Nonlinear Hyperspectral Unmixing Methods,” *IEEE J. Sel. Top. Appl. Earth Obs. Remote Sens.*, vol. 7, no. 6, pp. 1844–1868, June 2014.
- [35] J. Bioucas-Dias and M. Figueiredo, “Alternating direction algorithms for constrained sparse regression: Application to hyperspectral unmixing,” in *IEEE GRS Work. Hyperspectral Image Signal Process. Evol. Remote Sens. (WHISPERS)*, June 2010, pp. 1–4.